

# Heavy Quark Charge Asymmetries With the CELLO Detector

C. Kiesling

Max-Planck-Institut für Physik und Astrophysik



## ABSTRACT

The production of  $b$  and  $c$  quarks in  $e^+e^-$  annihilation has been studied with the CELLO detector in the range from 35 GeV up to the highest PETRA energies. The heavy quarks have been tagged by their semileptonic decays. The charge asymmetries for  $b$  quarks at 35 and 43 GeV have been found to be  $A_{FB}^b = -(22.2 \pm 7.7 \pm 3.5) \%$  and  $A_{FB}^b = -(49.1 \pm 16.0 \pm 5.0) \%$ , respectively, using a method incorporating correlated jet variables for the separation of the heavy quarks from the background of the lighter quarks. The results are in agreement with the expectations from the standard model. The axial vector coupling constants of the heavy quarks  $c$  and  $b$  are found to be  $a_c = +(0.26 \pm 0.51)$  and  $a_b = -(1.21 \pm 0.44)$  taking  $B^0 - \overline{B}^0$  mixing into account.

## 1. Introduction

In the standard model of electroweak interactions the  $e^+e^-$  annihilation into a pair of elementary fermions, i.e. leptons or quarks, is uniquely determined by their electric charge and their weak isospin. For leptons, which are observable particles, the predictions of the standard model, in particular the sign, magnitude and the energy dependence of the charge asymmetry, have been impressively verified. As to the quarks, the measurement of the pair production cross section for a given quark flavour is complicated by the fact that free quarks do not exist but rather fragment into jets of hadrons. One therefore has to separate multihadronic final states due to a specific parent quark-antiquark pair from the competing background due to the other quark flavours ("flavour tagging").

Heavy quarks are customarily tagged by either requiring a semileptonic decay leading to a lepton with high transverse momentum  $p_T$  with respect to a suitably chosen event axis, or by explicitly reconstructing a meson carrying a definite quark flavour and charge. While meson tagging is very selective but suffers from low efficiency and is virtually impossible for  $b$  quarks far above threshold, lepton tagging is more efficient but less selective and suffers from substantial background contributions. These facts have seriously limited the accuracy of the measurements of heavy quark production in  $e^+e^-$  annihilation.

In this letter we report on measurements of the charge asymmetries and the semileptonic branching ratios for  $c$  and  $b$  quarks employing, in addition to the lepton  $p_T$ , some specifically selected jet variables for improved separation of the heavy quark from the competing backgrounds. A likelihood method is used to simultaneously determine the observables by adjusting them to fit the experimental multi-dimensional distributions of the selected lepton and jet variables.

## 2. Experiment

The data were taken with the CELLO detector [1] at PETRA at a fixed centre of mass energy of  $\sqrt{s} = 35$  GeV ( $\int \mathcal{L} dt = 87 \text{ pb}^{-1}$ ) and in the range between 38 GeV and 46.78 GeV ( $< \sqrt{s} > = 43$  GeV,  $\int \mathcal{L} dt = 42.7 \text{ pb}^{-1}$ ). Charged particles are measured over 91 % of the full solid angle in a cylindrical wire chamber assembly inside a 1.3 T magnetic field with a transverse momentum resolution of  $\sigma_{p_T}/p = 2\%p$  ( $p$  in GeV/c). The energy deposition of charged and neutral particles is measured in the barrel part of a fine-grain lead-liquid argon calorimeter, equipped with 19 planes of readout strips in three different orientations, covering 86 % of  $4\pi$ . The energy resolution of the calorimeter is  $\sigma_E/E = 0.05 + 0.10/\sqrt{E}$  ( $E$  in GeV). The angular resolution, assuming the interaction point as origin, is 6 to 10 mrad. Muons are detected in 92 % of  $4\pi$  with planar drift chambers which are mounted behind the magnet yoke of 80 cm of iron. The spatial resolution of 0.6 cm obtained with these chambers is matched to the positional uncertainty due to multiple scattering of the muons passing the hadron absorber.

**Table 1.** Identified lepton candidates in the data and expectations for signal and backgrounds from a full Monte Carlo simulation of the experiment. The input branching ratios for the Monte Carlo are  $Br_{MC}(c \rightarrow l) = 8.8\%$  and  $Br_{MC}(b \rightarrow l) = 12.2\%$ .

$\sqrt{s}$	electron selection		muon selection	
	35 GeV	43 GeV	35 GeV	43 GeV
lepton candidates	940	374	806	453
lepton ident. eff.	86.2 %	85.4 %	77.3 %	63.6 %
hadron misident. prob.	2.49 %	2.44 %	2.54 %	1.33 %
MC expectation	967.5	368.1	828.1	393.2
$b \rightarrow l$	10.6 %	10.4 %	17.3 %	13.6 %
$b \rightarrow c \rightarrow l$	3.8 %	3.9 %	4.1 %	5.3 %
$c \rightarrow l$	17.4 %	15.1 %	29.9 %	22.8 %
$b \rightarrow$ hadrons	7.4 %	7.9 %	6.1 %	8.2 %
$c \rightarrow$ hadrons	24.1 %	23.7 %	20.0 %	23.0 %
$uds$ hadrons	35.5 %	37.7 %	22.6 %	27.1 %
DIS/IC	1.2 %	1.3 %	0 %	0 %

The analysis starts from a data sample of multihadronic events selected according to criteria described previously [2]. Additional cuts on the sphericity ( $> 0.025$ ) and the polar angle for the thrust axis ( $\cos \theta < 0.65$ ) were applied in order to reduce background not well described by the Monte Carlo simulation. The total data sample consists of 24216 (8473) events at  $\sqrt{s} = 35$  (43) GeV, respectively. Background from cosmic rays, beam gas,  $\tau^+\tau^-$ , and other QED events was determined to be less than 3 %.

### 3. Lepton Identification

In the multihadronic event sample, electrons were identified as charged particles with momentum greater than 1 GeV/c, with an energy deposit in the calorimeter matching the momentum measurement and a longitudinal and lateral energy distribution compatible with that from an electromagnetic shower. Details of the likelihood ratio technique used to tag the electron are given elsewhere [3]. The efficiency of identifying electrons was determined by Monte Carlo calculations to about 86 %, with a hadron misidentification probability of 2.5 %. Deep-inelastic electron photon scattering and inelastic Compton scattering background was further reduced by requiring substantial jet activity in the electron hemisphere. The number of electron candidates and the respective fractions from the various sources, as determined by a detailed Monte Carlo

simulation of the experiment, are shown in Table 1. For the calculations the semileptonic decay branching ratios  $Br(b \rightarrow l) = 12.2\%$  and  $Br(c \rightarrow l) = 8.8\%$  have been assumed.

The muon identification is based on their range, using the space points reconstructed in the muon chambers. Two variables are employed to evaluate a track-hit association: The distance  $d$  between a reconstructed hit and the track extrapolated from the central detector and the quality  $Q$ , defined as the ratio of the distance  $d$  over the uncertainty in the extrapolation [3]. All muon candidates had to exceed a minimum momentum of  $1.6 \text{ GeV}/c$  in order to penetrate the iron absorber. As for the electron case, the observed number of muon candidates and the expected backgrounds are shown in Table 1.

## 4. Flavour Separation

Semileptonic decays of the heavy quarks  $b$  ( $c$ ) can be enhanced over the background of competing light quark decays by requiring a minimum (maximum) transverse momentum  $p_T$  of the decay lepton with respect to the event axis using the thrust or sphericity variable [4, 5–8]. As was shown previously [6, 9], the separation of  $c$  and, in particular, of  $b$  quarks from the light-quark background can be substantially improved using additional event shape variables reflecting the mass difference between these quarks. JADE [6], e. g., have chosen the transverse jet mass and the missing transverse momentum partly due to the presence of high energy neutrinos in the semileptonic decays.

We have investigated many such variables (details of this analysis are described elsewhere [3]) and found that in addition to the transverse momentum  $p_T$  of the lepton the sum of the momenta  $\sum p_T^{\text{out}}$  of all particles perpendicular to the event plane (similar to the “transverse” mass used by JADE) and the variable  $E_{\text{corr}}$ , first introduced by the PLUTO collaboration [7], provide optimal separation. The dimensionless variable  $E_{\text{corr}}$  is the total energy of all particles inside a given cone around the direction of the lepton candidate, divided by the visible energy. For our experimental conditions, the optimum half angle of the cone was found to be 10 degrees. In contrast to JADE and PLUTO, the lepton momenta are included in the definition of both variables. The separating power of these variables was studied on the basis of Monte Carlo calculations, both at the four-vector level, using the  $O(\alpha_s^2)$  LUND 5.2 generator [10], and for the full detector simulation. Examples for the distributions of the three most powerful discriminating variables are shown in Fig. 1 at the four-vector level and in Fig. 2 for the full detector simulation, using the muon channel at a centre of mass energy of 35 GeV. While the distributions for  $b$  quarks show good separation, one notices that the  $c$  quarks strongly overlap with the background from the light quarks.

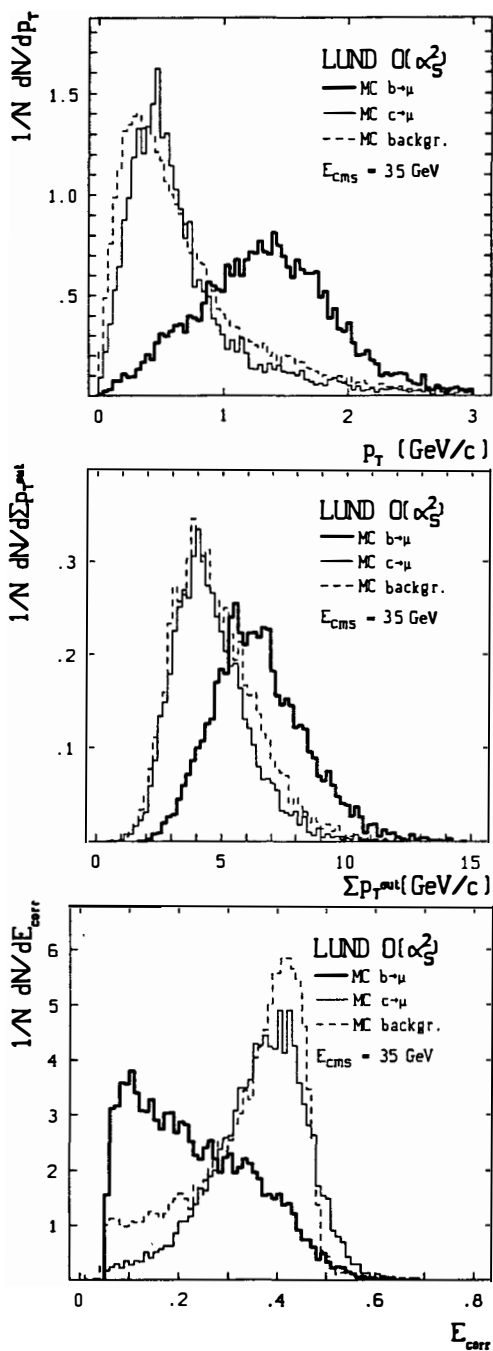


Fig. 1. Monte Carlo expectations for the three discriminating variables at the four-vector level ("ideal" detector). The individual contributions are normalised to the same area.

## 5. Analysis Method

We have chosen to simultaneously determine the semileptonic branching ratios and the charge asymmetries for  $b$  and  $c$  quarks from a fit to the observed distributions of the discriminating variables  $p_T$ ,  $\sum p_T^{\text{out}}$  and  $E_{\text{corr}}$ . The likelihood function is given by

$$\begin{aligned} \mathcal{L} = \prod_{i=1}^N & \left\{ f^b \rho^b(p_T, \sum p_T^{\text{out}}, E_{\text{corr}}) \left[ \frac{3}{8}(1 + x_i^2) + A_{\text{FB}}^b x_i \right] \right. \\ & + f^c \rho^c(p_T, \sum p_T^{\text{out}}, E_{\text{corr}}) \left[ \frac{3}{8}(1 + x_i^2) - A_{\text{FB}}^c x_i \right] \\ & \left. + f^{\text{bg}} \rho^{\text{bg}}(p_T, \sum p_T^{\text{out}}, E_{\text{corr}}) \left[ \frac{3}{8}(1 + x_i^2) + A_{\text{FB}}^{\text{bg}} x_i \right] \right\}, \end{aligned} \quad (1)$$

where the dependence on  $x = \cos \theta_{\text{jet}}$  is suggested by the expectation of the standard model. The following normalisation condition for the fractions of  $b \rightarrow l$  decays ( $f^b$ ),  $c \rightarrow l$  decays ( $f^c$ ) and background events ( $f^{\text{bg}}$ ) in the number  $N$  of identified leptons is used:

$$f^b + f^c + f^{\text{bg}} = 1 \quad (2)$$

with

$$f^{\text{bg}} = f^{\text{had}} + f^{bc}.$$

The fractions  $f^i$  are related to the semileptonic branching ratios  $Br_i$ , the branching ratios  $Br_i(\text{MC})$  input to the Monte Carlo simulation and the expected signal  $N_{\text{MC}}^i$  by

$$Br_i = \frac{N f^i}{N_{\text{MC}}^i} Br_i(\text{MC})$$

The asymmetry of the background due to  $b \rightarrow c \rightarrow l$  decays ( $f^{bc}$ )

$$A_{\text{FB}}^{\text{bg}} = -\frac{f^{bc}}{f^{\text{bg}}} A_{\text{GSW}}^b$$

has been determined from Monte Carlo and is found to be  $\leq 3\%$ .

In the likelihood fit the fraction  $f^b$  and the charge asymmetries  $A_b$  and  $A_c$  were treated as free parameters. The density functions  $\rho(p_T, \sum p_T^{\text{out}}, E_{\text{corr}})$  and the background contribution  $f^{\text{bg}}$  were taken from Monte Carlo. Note that the density function  $\rho$  is a 3-dimensional distribution (with projections shown in Fig. 1, 2) and thus takes advantage of the full correlation of the separating variables. For practical reasons we used binned distributions with a typical number of 30 bins in each dimension.

The essential point in the Monte Carlo investigations was to study the effects of the additional jet variables on the semileptonic branching ratios, charge asymmetries and their errors.

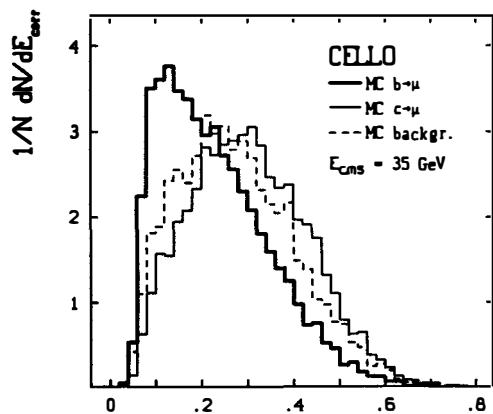
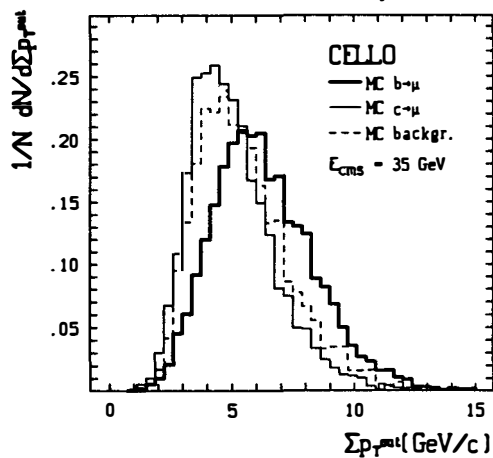
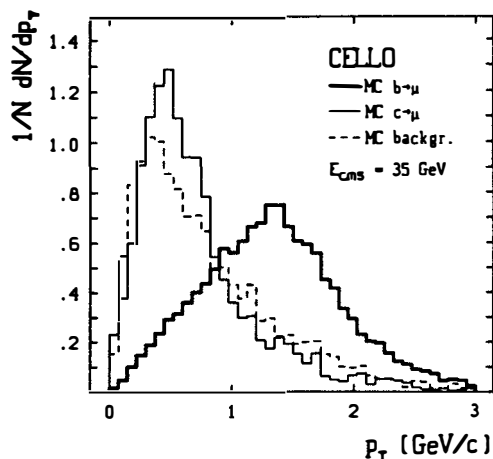


Fig. 2. Monte Carlo expectations for the three discriminating variables including a full simulation of the detector. The individual contributions are normalised to the same area.

**Table 2.** Results of the Monte Carlo study for the charge asymmetry and the signal fraction of  $b$  quarks at 35 GeV, tagged by muons, as functions of an increasing number of discriminating variables (see text). The numbers given are based on 40000 events for the four-vector (generator) study and on 4000 events with full detector simulation, selected from a sample of 100000 generated multihadronic events.

	LUND generator		detector simulation	
	$A_{FB}^b$ [%]	$f^b$ [%]	$A_{FB}^b$ [%]	$f^b$ [%]
$p_T$	$-(22.0 \pm 2.0)$	$22.3 \pm 0.39$	$-(24.2 \pm 8.7)$	$19.8 \pm 1.5$
$p_T \otimes \sum p_T^{\text{out}}$	$-(18.7 \pm 1.8)$	$22.2 \pm 0.34$	$-(26.0 \pm 6.2)$	$19.9 \pm 1.0$
$p_T \otimes \sum p_T^{\text{out}} \otimes E_{\text{corr}}$	$-(18.4 \pm 1.5)$	$22.3 \pm 0.29$	$-(27.0 \pm 4.2)$	$19.8 \pm 0.7$
MC input	$-(22.7 \pm 1.3)$	22.3	$-(29.0 \pm 4.0)$	19.9

**Table 3.** Statistical errors of the  $b$  quark charge asymmetry at 35 GeV in the data and for the expectation from a full detector simulation and a four-vector Monte Carlo, as functions of an increasing number of discriminating variables (see text). The  $b$  quarks have been tagged by muons. The statistics in the Monte Carlo is chosen to match the number of muon candidates in the data (806 events)

$\Delta A_{\text{stat}}^b$	data	detector simulation	LUND generator
$p_T$	21 %	20 %	14 %
$p_T \otimes \sum p_T^{\text{out}}$	15 %	15 %	11 %
$p_T \otimes \sum p_T^{\text{out}} \otimes E_{\text{corr}}$	10 %	10 %	10 %

In particular, Monte Carlo data were used at the four-vector level and including the detector simulation in order to determine the asymptotic (ideal detector) and the expected (real detector) results. Starting from using only  $p_T$  as discriminating variable, further variables ( $\sum p_T^{\text{out}}, E_{\text{corr}}$ ) were added and fitted for the charge asymmetries. The results of this investigation for the charge asymmetry of the  $b$  quark  $A_{FB}^b$  and the fractions  $f^b$  are shown in Table 2. While the central value of  $A_{FB}^b$  is stable upon variation of the number of discriminators, one observes that the inclusion of the additional jet variables and their correlations improves the error considerably, as is shown in Table 3.

It was furthermore observed that stable results for the charge asymmetry could only be obtained taking into account the full correlation of variables in the density functions  $\rho$ : Using instead a product ansatz of the individual projections leads to systematic shifts of  $A_{FB}^b$  towards lower absolute values with an increasing number of event shape variables. This result is verified both on the four-vector and the detector simulation level. With the multi-dimensional correlation functions  $\rho$ , on the other hand, we are able to reproduce the charge asymmetries and



**Table 4.** Measurements of the semileptonic branching ratios of  $c$  and  $b$  quarks, separately for the two lepton channels and centre-of-mass energies. Averages for the leptonic branching ratios from all energies are also given.

$\sqrt{s}$	channel	branching ratio [%] charm	branching ratio [%] bottom
43 GeV	$q \rightarrow e$	$9.2 \pm 1.4 \pm 2.0$	$11.1 \pm 2.8 \pm 2.6$
43 GeV	$q \rightarrow \mu$	$11.4 \pm 1.0 \pm 1.3$	$10.4 \pm 2.3 \pm 1.6$
43 GeV	$q \rightarrow l$	$10.7 \pm 0.8 \pm 1.7$	$10.6 \pm 1.8 \pm 2.1$
35 GeV	$q \rightarrow e$	$6.9 \pm 0.5 \pm 1.1$	$15.0 \pm 1.1 \pm 2.2$
35 GeV	$q \rightarrow \mu$	$7.2 \pm 0.4 \pm 0.6$	$14.8 \pm 1.0 \pm 1.6$
35 GeV	$q \rightarrow l$	$7.1 \pm 0.3 \pm 0.7$	$14.8 \pm 0.8 \pm 1.9$
$\langle \rangle$	$q \rightarrow l$	$7.8 \pm 0.81$	$13.3 \pm 1.63$

event fractions input to our simulations (see Table 2). We attribute this fact to the superior separating ability when the full correlation is taken into account.

We have also calculated the expected errors of  $A_{FB}^b$  based on our experimental statistics (see Tables 1 and 4 below). The resulting values are shown in Table 3 as functions of increasing number of discriminating variables. The expectations from the full Monte Carlo are in good agreement with the actual errors in the data. One can see that the errors are minimal for 3 variables as observed consistently in the high statistics Monte Carlo studies and in the data. Furthermore, the smearing due to the imperfect particle detection has no consequence for the asymmetry error, which is around 10 % for the best case (see Table 3).

## 6. Results

With a method optimised as described the semileptonic branching fractions and the charge asymmetries were simultaneously determined for the  $b$  and  $c$  quarks in each of the two leptonic channels at 35 and 43 GeV. The results of the fits to the  $p_T$ ,  $\sum p_T^{\text{out}}$  and  $E_{\text{corr}}$  distributions are shown in Fig. 3 together with the experimental data. Good agreement of the model calculations with the data is observed. The numerical results of the semileptonic branching fractions and charge asymmetries are shown in Table 4 and 5, respectively. Note that  $f^c$  is calculated from the normalisation condition in (2). Both the statistical (first) and systematic (second) errors are given. We find good agreement of the semileptonic branching ratios with previous experiments [11, 12].

**Table 5.** Measurements of the charge asymmetries for  $c$  and  $b$  quarks, separately for each lepton channel and centre-of-mass energy. The charge asymmetries for the  $b$  quarks are corrected to the Born level (see text).  $B^0 - \bar{B}^0$  mixing has not been taken into account.

$\sqrt{s}$	channel	lepton cand. signal	$A_{FB} [\%]$	$A_{\text{GSW}}^{\text{Born}} [\%]$
43 GeV	$c \rightarrow e$	374 (58)	$-(22.2 \pm 26.7 \pm 5.0)$	
43 GeV	$c \rightarrow \mu$	453 (116)	$+(18.5 \pm 15.5 \pm 5.0)$	
43 GeV	$c \rightarrow l$	827 (174)	$+(7.7 \pm 13.4 \pm 5.0)$	-21.6
43 GeV	$b \rightarrow e$	374 (35)	$-(44.6 \pm 27.6 \pm 6.0)$	
43 GeV	$b \rightarrow \mu$	453 (45)	$-(51.3 \pm 19.7 \pm 4.0)$	
43 GeV	$b \rightarrow l$	827 (80)	$-(49.1 \pm 16.0 \pm 5.0)$	-38.9
35 GeV	$c \rightarrow e$	940 (132)	$-(14.1 \pm 13.0 \pm 6.0)$	
35 GeV	$c \rightarrow \mu$	806 (203)	$-(12.2 \pm 9.7 \pm 5.0)$	
35 GeV	$c \rightarrow l$	1746 (335)	$-(12.9 \pm 7.8 \pm 5.5)$	-13.3
35 GeV	$b \rightarrow e$	940 (126)	$-(21.0 \pm 11.8 \pm 4.0)$	
35 GeV	$b \rightarrow \mu$	806 (173)	$-(23.0 \pm 10.2 \pm 3.0)$	
35 GeV	$b \rightarrow l$	1746 (299)	$-(22.2 \pm 7.7 \pm 3.5)$	-25.6

The charge asymmetries in Table 5 have been corrected for electroweak radiative effects up to the one-loop level [13,14]. Furthermore,  $O(\alpha_s)$  QCD corrections and mass effects [15] have been taken into account. The total corrections to the  $b$  ( $c$ ) quark asymmetry at 35 and 43 GeV amount to +2.8 % and +3.25 % (-1.9 % and -1.4 %), respectively [3]. Our measurements include the first determinations of the heavy quark charge asymmetries at 43 GeV. The value for  $A_{FB}^b$  at 35 GeV is in good agreement with the only other measurement significantly different from zero, done by JADE [6] at the same centre-of-mass energy.

The systematic errors have been estimated by varying the main parameters entering the fitting procedure. Most importantly, we varied the fragmentation parameters of the Peterson function [16] for the heavy quarks between conservatively wide limits, from the world averages  $\epsilon_b = 0.012, \epsilon_c = 0.09$  [17] used in the standard Monte Carlo to the “hard” values  $\epsilon_b = 0.0035, \epsilon_c = 0.025$ . The systematic error is dominated by this contribution. We also varied the criteria for the lepton identification, resulting in efficiencies between 70 and 88 % with correspondingly varying fractional background contributions. Furthermore, the number

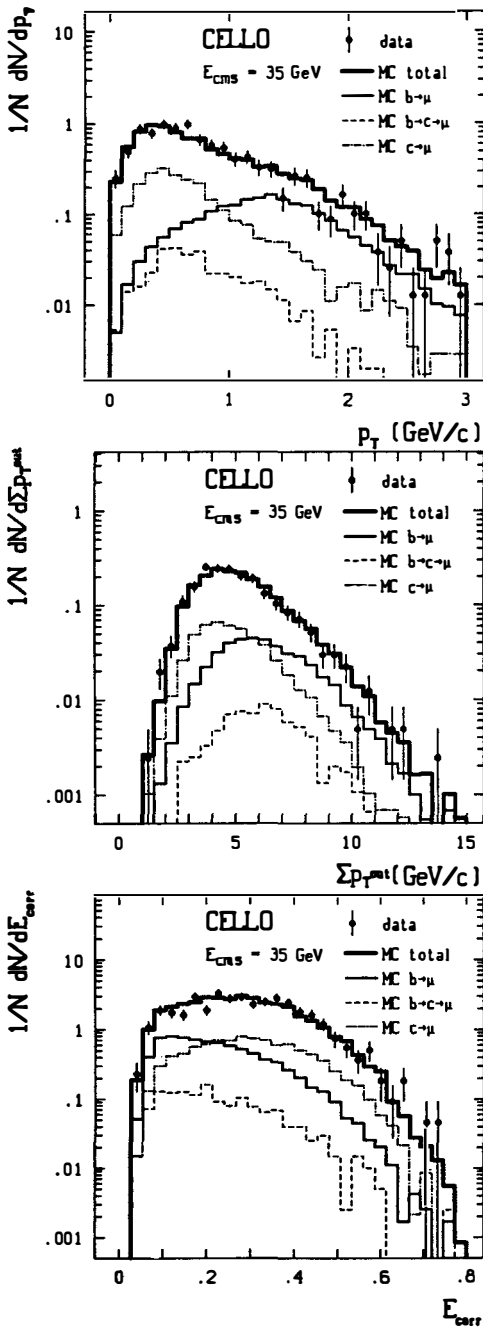


Fig. 3. Distributions for the three discriminating variables for the  $\mu$  candidate sample (data points). The histograms show the results of the fit and the expectations for the  $b$  and  $c$  quarks and the contribution of the background.

of bins for the density functions was varied between 20 and 30, limited on the lower side by the loss of separating power of the variable and on the high side by the available Monte Carlo statistics. The background contribution  $f^{\text{bg}}$  (including the contribution  $b \rightarrow c \rightarrow l$ , determined from Monte Carlo) was varied by  $\pm 10\%$  and turned out to be insensitive to the results. Finally we studied the influence of the experimental cut for the jet axis which was varied between  $0.5 < |\cos \theta_{\text{jet}}(\text{cut})| < 0.80$ . Fits were repeated for each of the above variations and the standard deviations of the resulting distributions for the asymmetries and branching ratios, weighted with their statistical errors, were determined. These standard deviations were taken as the systematic errors and are shown in Tables 4 and 5.

## 7. Determination of the Axial-Vector Charges

The values for the charge asymmetries of  $b$  and  $c$  quarks given in Tables 4 and 5 are corrected to the Born level of the standard theory, where they are given by

$$A_{\text{FB}}^q = \frac{3}{4} \frac{C_2}{C_1}$$

with

$$\begin{aligned} C_1 &= Q_c^2 Q_q^2 + Q_c Q_q v_e v_q \text{Reg}(s) + \\ &\quad \frac{1}{4} (v_e^2 + a_e^2) (v_q^2 + a_q^2) |g(s)|^2 \\ C_2 &= Q_c Q_q a_e a_q \text{Reg}(s) + v_e v_q a_e a_q |g(s)|^2 \\ g(s) &= \frac{1}{8 \sin^2 \theta_W \cos^2 \theta_W} \frac{s}{s - M_Z^2 + i M_Z \Gamma_Z} \end{aligned} \quad (3)$$

This expression can be used to determine the axial-vector charges  $a_q$  of the  $b$  and  $c$  quarks ( $q = b, c$ ), once the electric charges  $Q_q$  are inserted, the standard model predictions for the vector charges  $v_q$  are assumed, and the mass of the  $Z^0$  and the value of the Weinberg angle are chosen ( $M_Z = 92 \text{ GeV}$ ,  $\sin^2 \theta_W = 0.23$ ). Table 6 shows the results for the axial-vector charges separately for each lepton channel and centre of mass energy. The values for  $a_e$  are directly obtained from (3) and the measurements in Table 5. For the case of the  $b$  quark, however, one further correction to the charge asymmetry is necessary due to  $B^0 - \bar{B}^0$ -mixing, which reduces the observed charge asymmetry. With the measured value for the mixing parameter  $\chi_I = 0.10 \pm 0.03$  [18] the  $b$  quark charge asymmetries at the Born level  $A_{\text{GSW}}^b$  are determined from the measurements  $A_{\text{obs}}^b$  by

$$A_{\text{FB}}^b = \frac{1}{1 - 2\chi_I} A_{\text{obs}}^b$$

Inserting this expression into (3) yields the values for  $a_b$  in Table 6 with mixing. One should note that neglecting the purely weak terms in (3), as is usually done for lepton pair production

**Table 6.** Determinations of the axial-vector charges  $a_b$  ( $a_c$ ) of  $b$  ( $c$ ) quarks from the two lepton channels and centre-of-mass energies.  $a_b$  is given with and without  $B^0 - \bar{B}^0$  mixing (see text). The errors are statistical (first) and systematic (second). Averages over all lepton channels and energies have also been calculated. The uncertainties of the averages are obtained by adding the statistical and systematic errors in quadrature.

$\sqrt{s}$	channel	$a_c$	$a_b$ without mixing	$a_b$ with mixing
43 GeV	$q \rightarrow e$	$+(1.04 \pm 1.31 \pm 0.25)$	$-(1.19 \pm 0.94 \pm 0.20)$	$-(1.65 \pm 1.70)$
43 GeV	$q \rightarrow \mu$	$-(0.86 \pm 0.75 \pm 0.24)$	$-(1.44 \pm 0.79 \pm 0.16)$	$-(2.15 \pm 1.98)$
43 GeV	$q \rightarrow l$	$-(0.38 \pm 0.65 \pm 0.25)$	$-(1.34 \pm 0.60 \pm 0.18)$	$-(1.96 \pm 1.37)$
35 GeV	$q \rightarrow e$	$+(1.08 \pm 1.01 \pm 0.47)$	$-(0.82 \pm 0.48 \pm 0.16)$	$-(1.05 \pm 0.68)$
35 GeV	$q \rightarrow \mu$	$+(0.93 \pm 0.75 \pm 0.39)$	$-(0.90 \pm 0.42 \pm 0.12)$	$-(1.16 \pm 0.60)$
35 GeV	$q \rightarrow l$	$+(0.98 \pm 0.60 \pm 0.43)$	$-(0.87 \pm 0.32 \pm 0.14)$	$-(1.12 \pm 0.47)$
$\langle \rangle$	$q \rightarrow l$	$+(0.26 \pm 0.51)$	$-(0.98 \pm 0.31)$	$-(1.21 \pm 0.44)$

and also in most previous determinations of the axial couplings of the heavy quarks, will lead to inaccurate results for  $a_b$  and an underestimation of its error, with deviations at high energies and for large asymmetries sometimes in excess of 20 %.

Our determinations of the axial-vector coupling constants,  $a_b = -(1.21 \pm 0.44)$  (with mixing) and  $a_c = +(0.26 \pm 0.51)$ , are in good agreement with the expectation of the standard model and with other experiments. A compilation of the world data on  $a_b$  and  $a_c$  is shown in Figures 3 and 4, where the values for  $a_b$ ,  $a_c$  have been recalculated from the measured asymmetries [4, 5—7] using the full expression (3). It is interesting to note that the inclusion of the mixing improves the agreement with the standard model: Adding the CELLO data, the new world average without mixing is  $a_b = -(0.84 \pm 0.17)$ , whereas the value including mixing is  $a_b = -(0.98 \pm 0.22)$ , in perfect agreement with the expectation of  $a_b = -1$  (the MAC measurement [8], due to its positive charge asymmetry, cannot be used in the world average with  $B^0 - \bar{B}^0$  mixing and has therefore also been excluded for the calculation of  $a_b$  without mixing). Figures 4 and 5 show the compilations in graphical form.

The  $b$  asymmetry measurement can also be used to set a limit on  $\chi_I$ , assuming an expected asymmetry according to the standard model. One obtains  $\chi_I < 0.27$  (90 % C.L.). Using all PETRA data at 35 GeV the limit is  $\chi_I < 0.20$  (90 % C.L.).

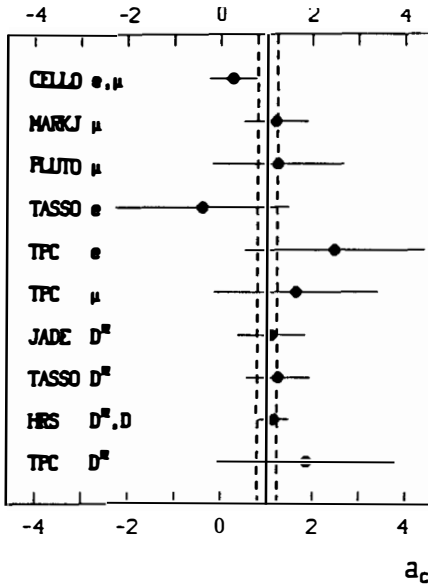


Fig. 4. Compilation of measurements for the axial-vector coupling for the  $c$  quark. The solid line corresponds to the new world average.

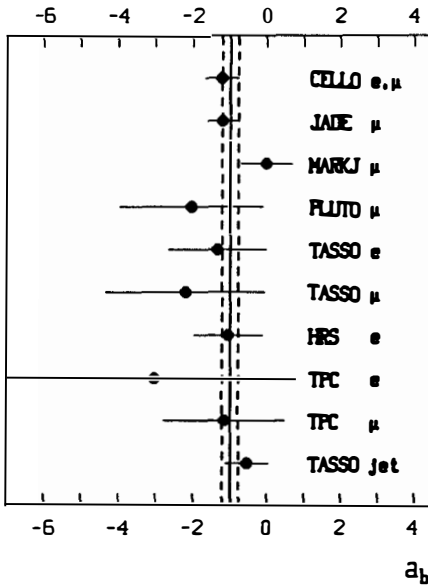


Fig. 5. Compilation of measurements for the axial-vector coupling of the  $b$  quark. The charge asymmetries  $A_{FB}^b$  from which the individual couplings are derived have been corrected for  $B^0 - \bar{B}^0$  mixing. The solid line corresponds to the new world average.

## 8. Conclusions

In conclusion, we have used the semileptonic decays of  $b$  and  $c$  quarks into electrons and muons to determine the charge asymmetries and the semileptonic branching ratios of these quarks. For the separation of the heavy quarks from the competing background of the light quarks we used, in addition to the transverse momentum of the lepton, suitably chosen jet variables. With Monte Carlo calculations we verified that the method produces stable results and that the uncertainties of the measured quantities (branching ratios and charge asymmetries) are substantially reduced. The charge asymmetry for  $b$  quarks,  $A_{FB}^b$ , is found to be  $A_{FB}^b = -(22.2 \pm 7.7 \pm 3.5) \%$  at 35 GeV, and  $A_{FB}^b = -(49.1 \pm 16.0 \pm 5.0) \%$  at 43 GeV. From these measurements we deduce an axial-vector coupling constant  $a_b$  in excellent agreement with the standard model expectation.

### Acknowledgement

I would like to thank J. Tran Thanh Van and J.-F. Grivaz for organising this pleasant and stimulating meeting. My special thanks go to H. Kroha for explaining to me many details of his analysis. The careful reading of the manuscript and the helpful suggestions by R. Kotthaus are gratefully acknowledged.

## References

- [1] CELLO Collab., H.J. Behrend et al., Physica Scripta 23 (1981) 610
- [2] CELLO Collab., H.J. Behrend et al., Phys. Lett. B193 (1987) 157
- [3] H.K. Kroha, Ph.D. thesis (1989), in preparation
- [4] HRS Collab., P. Baringer et. al., Phys. Lett. B206 (1988) 551; HRS Collab., C.R. Ng et. al., ANL-HEP-PR-88-11 (1988); TPC Collab., H. Aihara et. al., Phys. Rev. D31 (1985) 2719; Z. Phys. C27 (1985) 39; Phys. Rev. D34 (1986) 1945; JADE Collab., W. Bartel et al., Phys. Lett. B146 (1984) 121; MARK-J Collab., B. Adeva et al., Phys. Rep. 109 (1984) 133; TASSO Collab., M. Althoff et. al., Phys. Lett. B146 (1984) 443; Z. Phys. C22 (1984) 219
- [5] S.L. Wu, Proc. 1987 International Symposium on Lepton and Photon Interactions at High Energies, Hamburg (1987), p.39
- [6] JADE Collab., W. Bartel et al., Phys. Lett. B146 (1984) 437
- [7] C. Maxeiner, DESY PLUTO-85-03, internal report (1985)
- [8] MAC Collab., H.R. Band et al., Phys. Lett. B218 (1989) 369

- [9] R. Marshall, Z. Phys. C26 (1984) 26
- [10] B. Anderson et. al., Phys. Rep. 97 (1983) 33; Z. Phys. C20 (1983) 317; T. Sjostrand, Comp. Phys. Comm. 27 (1982) 243; Comp. Phys. Comm. 28 (1983) 229
- [11] DELCO Collab., D.E. Koop et al., Phys. Rev. Lett. 52 (1983) 970; HRS Collab., C.R. Ng et. al., ANL-HEP-PR-88-11 (1988); MAC Collab., B. Fernandez et al., Phys. Rev. Lett. 50 (1983) 2054; MARK II Collab., M.E. Nelson et al., Phys. Rev. Lett. 50 (1983) 1542; MARK II Collab., R.A. Ong et al., Phys. Rev. Lett. 60 (1988) 2587; TPC Collab., H. Aihara et al., Phys. Rev. D31 (1985) 2719; Z. Phys. C27 (1985) 39; JADE Collab., W. Bartel et al., Z. Phys. C33 (1987) 339; MARK-J Collab., B. Adeva et al., Phys. Rev. Lett. 51 (1983) 443; TASSO Collab., M. Althoff et al., Phys. Lett. B146 (1984) 443; Z. Phys. C22 (1984) 219
- [12] M. Sakuda, CALT-68-1138 (1984); B. Gittelman, S. Stone, CLNS 87/81 (1987); E.H. Thorndike, R.A. Poling, Phys. Rep. 157 (1988)
- [13] F.A. Berends, R. Kleiss, S. Jadach, Nucl. Phys. B202 (1982) 6
- [14] B.W. Lynn, R.G. Stuart, Nucl. Phys. B253 (1985) 216
- [15] J. Jersák, E. Laermann, P.M. Zerwas, Phys. Lett. B98 (1981) 363; Phys. Rev. D25 (1982) 1218
- [16] C. Peterson et. al., Phys. Rev. D27 (1983) 105
- [17] J. Chrin, Z. Phys. C36 (1987) 163
- [18] UA1 Collab., C. Albajar et. al., Phys. Lett. B186 (1987) 247; ARGUS Collab., H. Albrecht et. al., Phys. Lett. B192 (1987) 245; CLEO Collab., M. Artuso et. al., Phys. Rev. Lett. 62 (1989) 2233